IEEE P802.11
Wireless LANs

Alternative proposal for BRAN SYNCH preamble

(FOR INFORMATION ONLY)

Date: March 8, 1999

Author: Ralf Boehnke, Thomas Doelle
SONY International Europe GmbH
Stuttgarter Strasse 106, 70736 Fellbach, Germany
Phone: +49-711-5858-483
Fax: +49-711-5858468
e-Mail: boehnke@sony.de,
doelle@sony.de

Abstract

In this document we provide information on a proposal for PHY SYNCH preamble burst of HIPERLAN type 2 systems (ETSI BRAN project). The proposal was submitted to ETSI BRAN in the last meeting (BRAN#12.5) in Paris, 25-26 February 1999.
The document should be used as background information on SONY's BRAN synchronisation preamble proposal in ETSI BRAN.
The content is the same as in ETSI BRAN document 'HL12.5Son2a'.

1 Introduction

In this document we propose an appropriate structure to be used in the PHY SYNCH preamble burst of HIPERLAN type 2 systems. The construction suggested is independent of the burst content (e.g. OFDM type or other sequences) and improves the detection accuracy and receiver implementation flexibility. Furthermore extensive simulation results based on OFDM type content are provided to prove the applicability and improved performance of the structure. The proposal has a high commonality to the current IEE802.11 (draft) SYNCH burst structure

The current working assumption for the overall structure of the preamble is depicted in Figure 1-1, it consists of 3 different fields (A, B, C). In [1] a detailed proposal for the content of the H2 PHY SYNCH preamble is proposed (Figure 1-2).

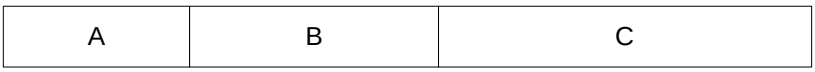

Figure 1-1 H2 PHY SYNCH preamble

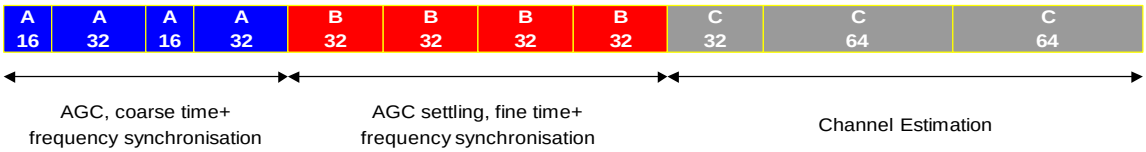

Figure 1-2 Preamble structure proposed by Ericsson/Nokia

The field A is considered for preamble detection, AGC setting and coarse timing and frequency synchronisation. Fine frequency tuning and fine timing is done using the B-Field. The C-Field is reserved for channel estimation.

2 Improved symbol structure of the A- field

The currently considered structure of the A-field is depicted in Figure 2-1 in detail. Coarse timing can be achieved through auto-correlation of the two repetitive patterns of length 48 or cross-correlation (length 32 or 48).

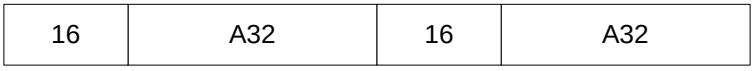

Figure 2-1 A-field as proposed WA

For improved preamble detection probability and time acquisition accuracy we propose to use the structure of the A-field as depicted in Figure 2-2. The length of the A-field is not changed by the alternative structure. It consists of 6 repetitive short OFDM symbols. The complex samples of the last short symbol are phase-shifted by 180°. There are several advantages given by using this structure. The granularity of the short symbols is higher, which leads to a larger correlation window in the case of auto-correlation. The shorter auto-correlation delay allows the detection of larger frequency offsets. On both structures a cross-correlation of length 32 can be applied. Overall the structure as depicted in Figure 2-2 gives more flexibility. Using this structure the precision of the coarse timing and the reliability of the preamble detection can be improved as shown in the next sections.

Figure 2-2 Improved structure of the A-field

3 Performance

3.1 Simulation Parameters and criteria for comparison

For the objective comparison basic simulation parameters and criteria for comparison have been agreed on the last BRAN meeting [2]. The used parameters are listed below:

- Channel Model: BRAN E [3] with uniformly distributed tap phases
- Frequency offset: 200 kHz (+/- 20ppm)
- MAC- frame duration: 2 ms
- Signal clipping: -20 dB (below signal mean), no clipping
- SNR: 5dB (low), 10dB (medium)

Simulations for the following criteria for comparison have been performed:

- Timing accuracy
- False alarm probability
  (false detection of preamble within data field of a MAC frame/ total number of frames)
- Detection failure
  (preamble was not detected within a MAC frame/ total number of frames)
- Correct preamble detection
  (preamble was detected within the preamble field **and** not detected within the data field of a MAC frame/ total number of frames)

3.2 Detection method

3.2.1 Auto-correlation

To show the improved acquisition reliability we want to consider the synchronisation using auto-correlation (AC), which is referred here to the delayed signal correlation as shown in Figure 3-1. The received signal is delayed by the correlation delay D_{ac}. The conjugate complex samples of the delayed version are multiplied with the received samples. The products are feed into the moving average of window size W_{ac} and are then post-processed for a threshold detection and/or maximum search to find the correct timing. The complex correlation result at the peak position can be used to estimate the frequency offset.

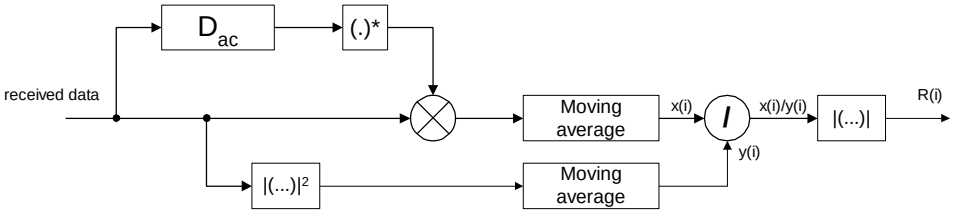

Figure 3-1 Auto-correlation block diagram

Table 3-1 lists the auto-correlation parameters for the different proposed structures of the A-field - *A32* (as shown in Figure 2-1), *A16_inv* (as shown in Figure 2-2). The maximum detectable frequency offset (F_{omax}) is 208.33 kHz in case of auto-correlation with *A32*.
Bearing in mind the frequency allocation of H/2 systems (5150MHz-5350MHz, 5470MHz-5725MHz, 5725MHz-5925MHz) as given in [4] the maximum frequency offset is **214kHz** (at 5350MHz), 229kHz (at 5750MHz) and 237kHz (at 5925MHz). Therefore the maximum detectable frequency offset range of 208.33kHz for structure *A32* is not sufficient. For *A32* an auto-correlation type receiver can not achieve a coarse frequency synchronisation taking into account an oscillator accuracy of ±20ppm. The structure *A16_inv* covers the possible frequency offset range with a large margin and a reliable coarse frequency synchronisation using auto-correlation based receiver is easily possible.

Structure	D_{ac}	W_{ac}	F_{omax} [kHz] *)
A32	48	48	208.33 !!
A16_inv	16	64	625

*) for 20 MHz sampling frequency, (I)FFT size of 64

Table 3-1 Auto-correlation parameters

Figure 3-2 shows the auto-correlator output for the different structures in the case of AWGN and multipath channel E. One can see the clear peaks in case of the AWGN-channel and broader peaks in the case of the multipath channel. The *A32* structure produces higher side lobes than the *A16inv* structure, which already indicates the possibility of a higher false alarm probability. Structure *A16inv* produces a clear peak with the lowest side lobes.

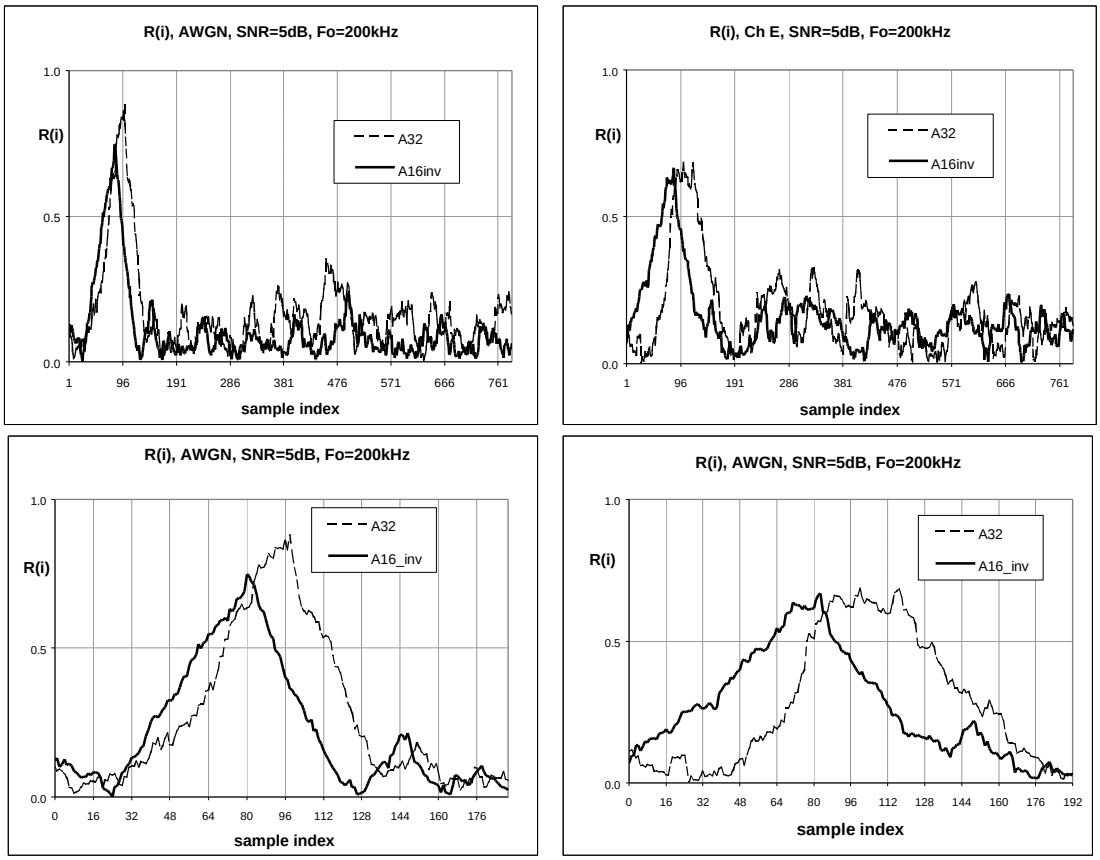

Figure 3-2 Correlator output R(i)

In the following statistical measurements regarding the timing accuracy, false alarms and detection failures are considered for comparison purposes. The timing accuracy is given by the timing error, which is measured in samples (+/-).

To specify the requirement on the coarse timing accuracy the duration of the used guard interval and the maximum delay spread of the multipath environment should be considered. Taking into account a duration of the guard interval of 800ns and the delay spread of 250ns of Channel BRAN E the accuracy that has to be achieved is within +/- 5 samples.

The simulations of the timing accuracy have been performed for 200 MAC frames each of 2ms duration. The results are depicted in Figure 3-3 to Figure 3-5. In the case of signal clipping 20 dB below the mean signal level and a SNR of 5dB (Figure 3-4) the current considered structure *A32* poorly satisfies the requirement as given above. A timing accuracy of +/-5 samples is only reached for about 70 % of the simulated received frames. Much more accurate results can be achieved with the structure *A16inv*. On the other hand a **tendency for false alarm can be recognised if the structure *A32* is used.** This will be verified considering the false alarm and detection failure probability.

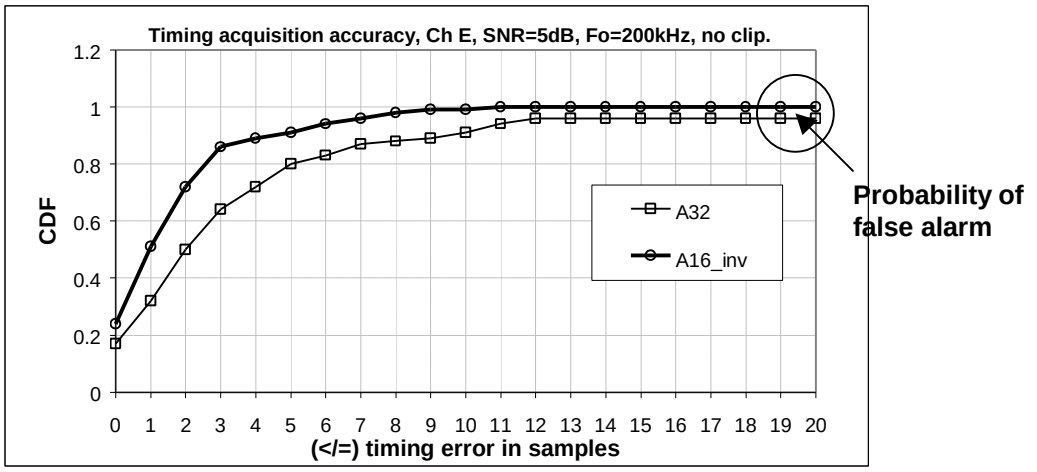

Figure 3-3 Timing acquisition accuracy measured in samples (ChE, 5dB, no clipping)

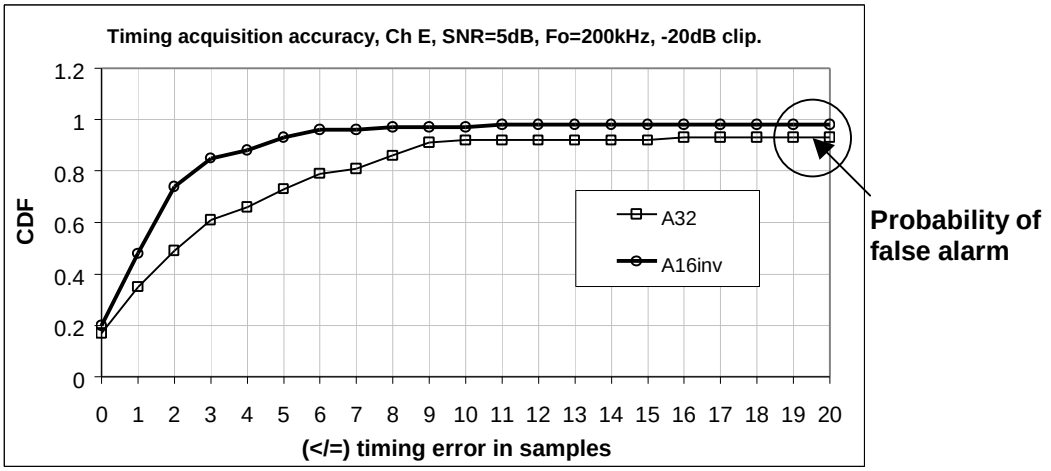

Figure 3-4 Timing acquisition accuracy measured in samples (Ch-E, 5dB, -20 dB clipping)

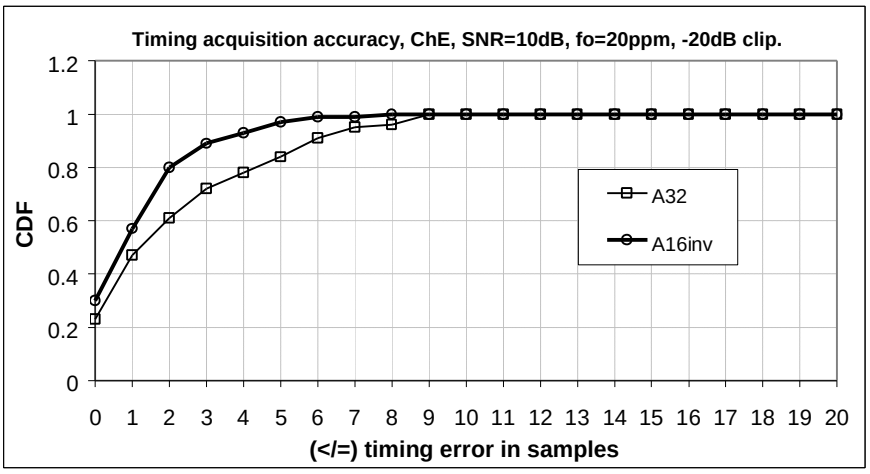

Figure 3-5 Timing acquisition accuracy measured in samples (Ch-E, 10dB, -20 dB clipping)

The false alarm is defined as an event when the preamble is detected within the data field of a MAC frame and the detection failure is defined as an event when the preamble is **not** detected within the preamble field of a MAC frame. The false alarm probability is measured depending on the adjusted threshold that the correlation result has to reach before timing is acquired.
Figure 3-6 and Figure 3-7 show the false alarm as well as the detection failure probability. The simulations have been performed for 2000 frames each of duration of 2.0ms. Where there is no major difference between the structures regarding the detection failure rate there is a significant advantage of structure *A16* over *A32* regarding the false alarm probability.

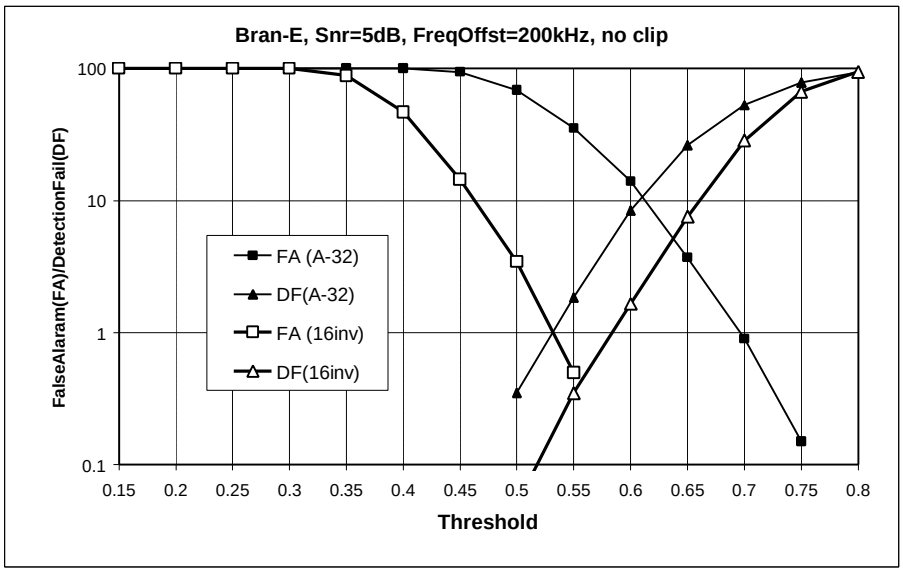

Figure 3-6 False alarm and Detection failure probability [%] (Ch-E, 5dB, no clipping)

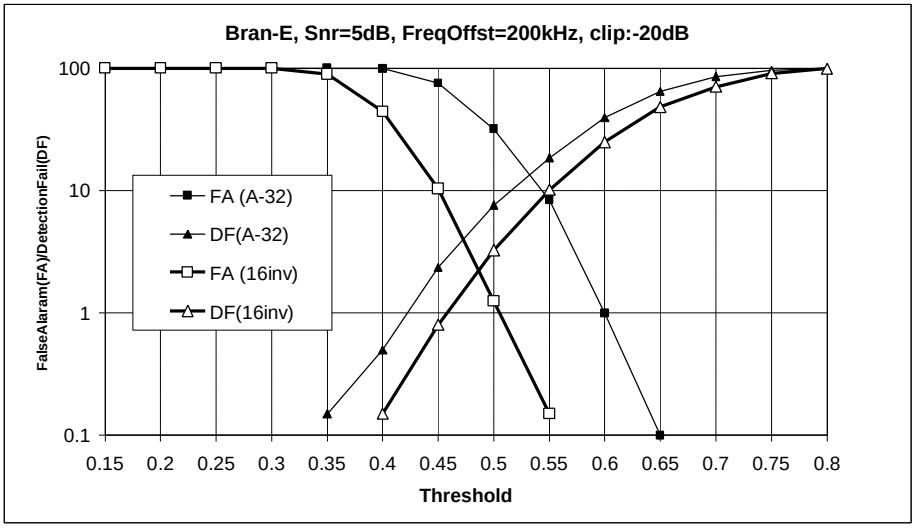

Figure 3-7 False alarm and Detection failure probability [%] (Ch-E, 5dB, -20dB clipping)

Comparison (Bran-E, Snr=5dB, Frequency Offset=200kHz, clip at –20dB from mean level)

At the threshold of 0.49 the structure *A16inv* achieves a False Alarm probability of 2.9% and a synch failure rate of 2.9%. At the threshold of 0.53 the structure A32 achieves a False Alarm probability of 14% and a synch failure rate of 14%.

Correct Detection Probability

We define the correct detection probability as the joint event of detecting the SYNCH preamble (correlation output exceeds the threshold within the SYNCH preamble) correctly and not exceeding the threshold within the data part of a MAC frame. The results are depicted in Figure 3-8 and Figure 3-9. The proposed structure *A16inv* outperforms A32 by 21% (*A16inv*: maximum of 95.5%, A32: maximum of 74.4%) in the worst case scenario (with clipping).

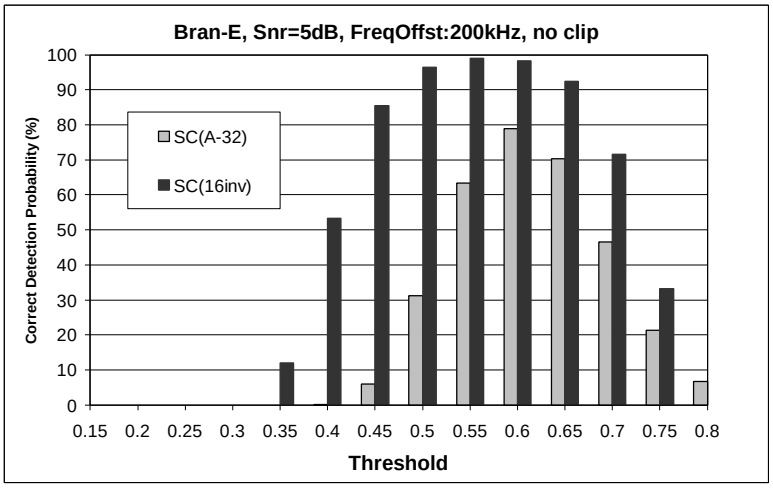

Figure 3-8 Correct Detection Probabilities (Bran-E, no clipping)

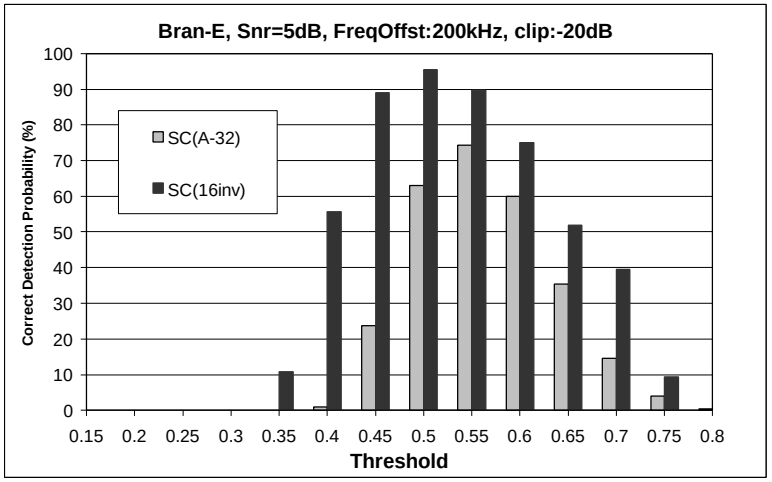

Figure 3-9 Correct Detection Probabilities (Bran-E, with clipping)

Implementation complexity

The implementation complexity depends on the resolution (bit per sample) and the auto-correlation structure, which is almost the same for A32 and *A16inv*. A generic comparison is possible if we assume that each complex sample uses two registers and a real sample needs one register.

Structure	**A32**		**A16inv**	
AC delay	48 (complex)	96 (real)	16 (complex)	32(real)
AC (MAV)	48 (complex)	96 (real)	64 (complex)	128 (real)
RSSI (MAV)	48 (real)	48 (real)	64 (real)	64 (real)
Total		**240 (real)**		**224 (real)**

Table 3-2 Implementation complexity

3.2.2 Cross-correlation

A cross-correlation is performed for the incoming signal with the known (expected) signal in the receiver. This requires higher processing load (in the case of the period 32 sequence 32 complex multiplication's and 32 additions per incoming sample are needed). The higher processing complexity should be justified with the better peak position detection.

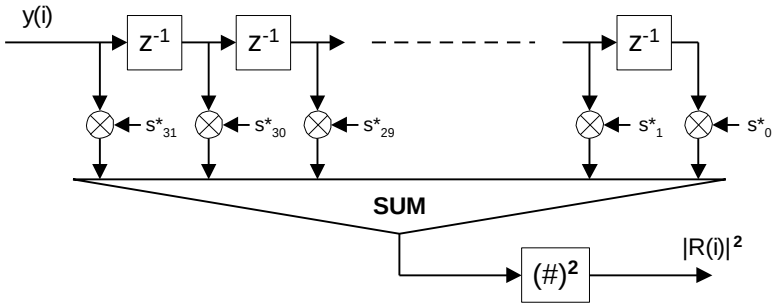

Figure 3-10: Cross Correlation Unit

In the simulations described below the cross-correlation was matched to A32 for the simulations with structure A32. For simulations of the structure *A16inv* the cross-correlation is matched to the last two patterns in the A-field of A16inv (non-flipped/flipped part).

Simulations have shown that cross-correlation over field A does not outperform auto-correlation to detect the SYNCH preamble (especially in fading environment where the expected cross-correlation peaks are 'smeared' over a number of samples due to the echoes of the channel). Cross-correlation should be used only to detect the B-field after rough timing acquisition was achieved and the expected cross-correlation peak positions are known.

In the following figures we depict the cross correlation start of a typical frame. It is visible that for Bran-E channel no secure threshold can be derived to distinguish the start of the SYNCH field from false alarms within the frame.

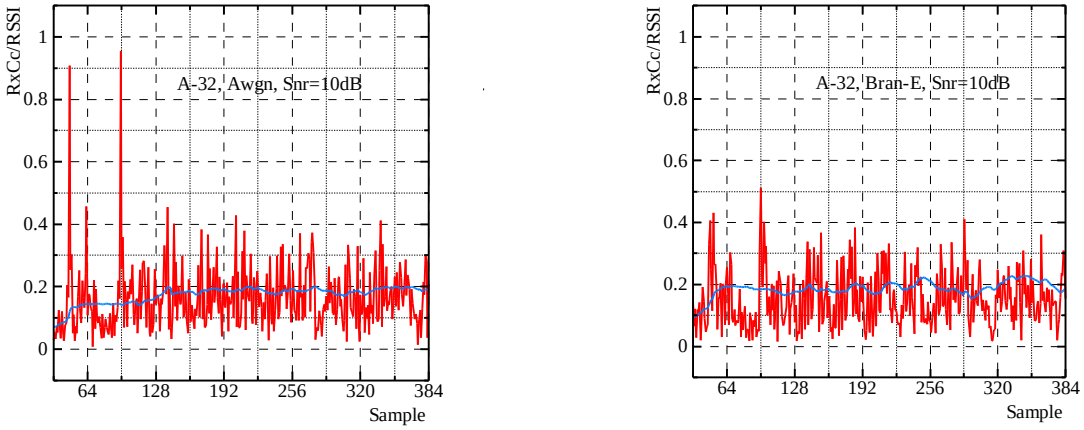

Figure 3-11 Output at cross-correlator for *A32* (AWGN, BRAN-E)

For the modified structure (A16inv) the same observations are valid (difficult definition of reliable threshold), however a long gap in front of the correlation peak exists. This gap may be used for pre-identifying the possible position of the cross-correlation peak (pre-synchronisation). Under ideal conditions (no fading channel, no noise) the cross-correlation results in the gap are exactly zero, it can still be detected under severe fading and noise.

The exploitation of the gap to be used for pre-synchronisation needs to be investigated further as an interesting feature of the structure *A16inv* proposed in this contribution. This special feature is not observed for the A32 structure.

In the sequel cross-correlation based detection is not considered for the following simulation results, as auto-correlation is a simpler and more obvious way for detection of the SYNCH preamble (A-field).

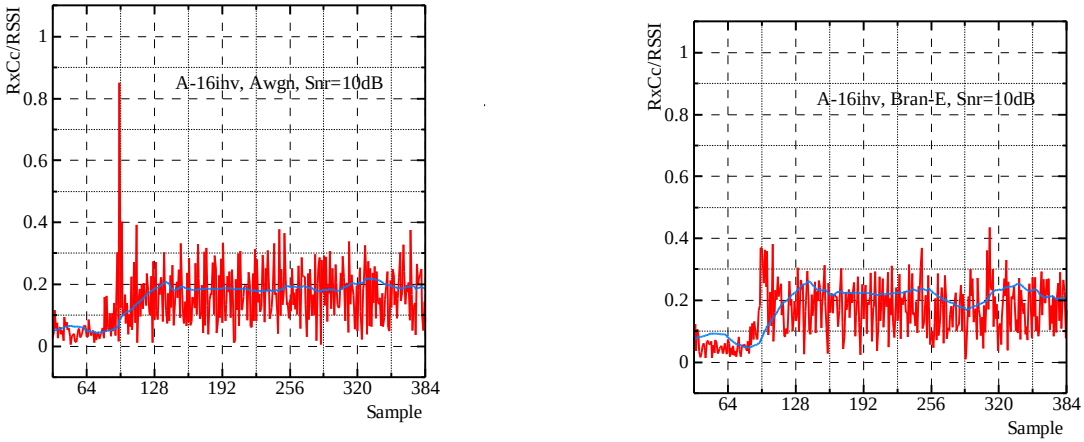

Figure 3-12 Output at cross-correlator for *A16inv* (AWGN, BRAN E)

Implementation flexibility

The structure *A16inv* can use a length-16 cross-correlation in environments with a smaller delay spread. Compared to the current IEEE802.11 the modification in *A16inv* provides a significant advantage, the last pattern ('A*') can be identified clearly when besides the peak (real value) the phase is observed. For the last pattern A* the peak has a phase shifted by 180 degrees compared to the peeks observed for 'A'.

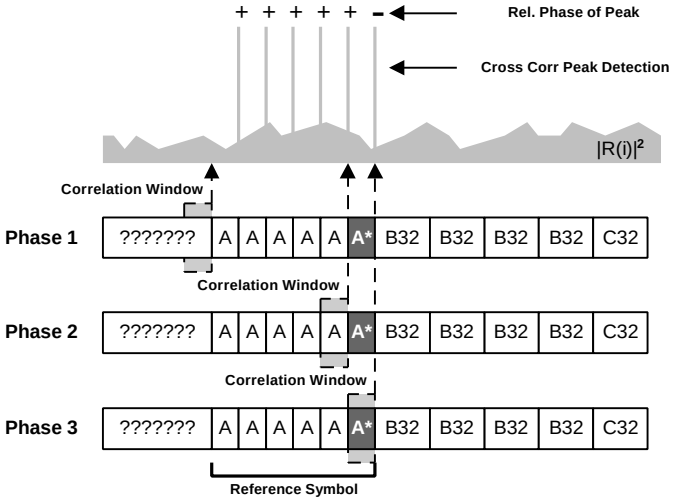

Figure 3-13 Cross-correlation (length 16) operation with *A16inv*

4 Time Domain Signal Properties

For OFDM (or in general multi-carrier signals) the signal envelope fluctuation (named Peak-to-Average-Power-Ratio = PAPR) is of great concern. A large PAPR results in poor transmission (due to non-linear distortion effects of the power amplifier) and other signal limiting components in the transmission system (e.g. limited dynamic range of the AD converter).

For synchronisation purposes it is even more desirable to have signals with a **low PAPR** and a **small dynamic range** in order to accelerate the receiver AGC (automatic gain control) locking and adjusting the reference signal value for the A/D converter. The whole dynamic range of the incoming signal should be covered by the A/D converter resolution without any overflow/underflow.

We propose a sequence for the generation of *A-16* that achieves a small PAPR and at the same time a small dynamic range (compared to the length 16 sequence in IEEE802.11).

4.1 Sequence generation

The sequence generation is similar to IEEE802.11 by modulation of every 4th subcarrier for a length 64 IFFT. The indices of the carriers modulated are –24, -20, … , -4, 4, 8, … , 24.
The symbol sequence is C0, C1, …, C11 and the mapping is:

$S_{-24..24}$=2*{ **C00**,0,0,0, **C01**,0,0,0, **C02**,0,0,0, **C03**,0,0,0, **C04**,0,0,0, **C05**,0,0,0, **0**,
0,0,0,**C06**, 0,0,0,**C07**, 0,0,0,**C08**, 0,0,0,**C09**, 0,0,0,**C10**, 0,0,0,**C11**}

	C00	C01	C02	C03	C04	C05	C06	C07	C08	C09	C10	C11
Seq-A16	+1+j	-1+j	-1-j	+1-j	-1-j	+1-j	+1-j	-1-j	+1-j	-1-j	-1+j	+1+j

The resulting time domain waveform has four periods (for 64 sample IFFT).

4.2 Sequence comparison

In the following graphs we analyse the properties of the sequence proposed and compare it to the current IEEE802.11 sequence. Oversampling is considered to capture the 'true' waveform (the effect of oversampling would appear in the real implementation as the result of the 'smoothening' low-pass filter after the D/A conversion at the transmitter side).

Signal (In and Quad part) using IEEE A-field sequence (8-times oversampling), four periods

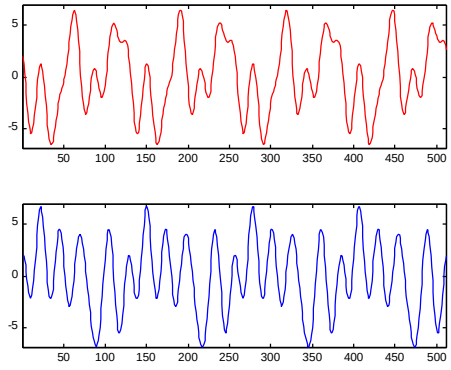

Signal (In and Quad part) using 'Seq-A16' (8-times oversampling) , four periods

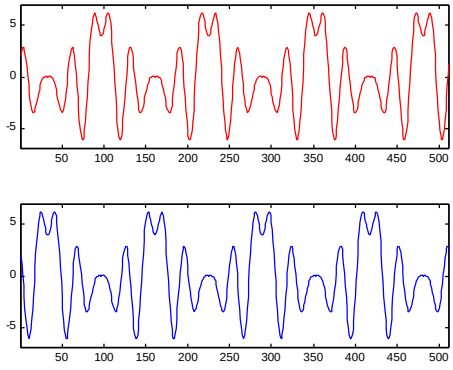

Original IEEE A-field
PAPR: 3.01dB
Dynamic Range: 30.82dB

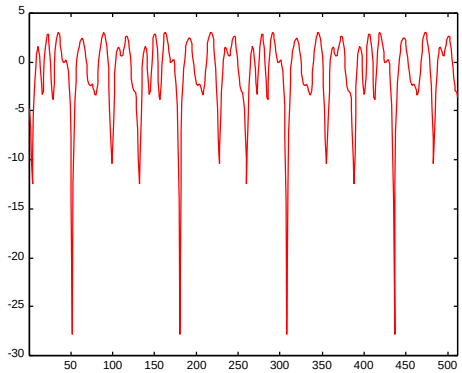

Modified Symbol Sequence for A-field
PAPR: 2.24dB
Dynamic Range: 7.01dB

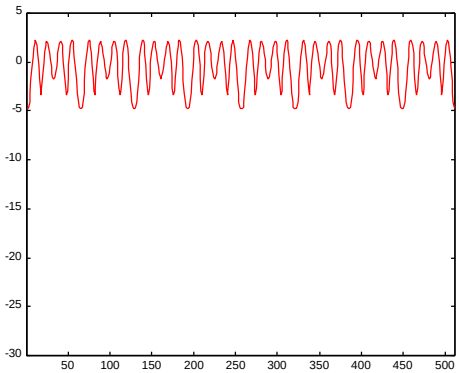

Compared to the sequence proposed for IEEE the PAPR is reduced from 3.01dB to 2.24dB and the dynamic range is reduced from 30.82dB to 7.01dB.

We cross-checked whether the sequence proposed achieves the same or better timing detection accuracy as the current IEEE802.11 length 16 sequence. The result in Figure 4-1 shows that the new sequence proposed outperforms the sequence from IEEE using the proposed A-field structure (besides the advantages of reduced PAPR and dynamic range).
We therefore conclude that the sequence proposed for field *A16_inv* achieves a low peak-to-mean-power-ratio, a small dynamic range and good detection performance.

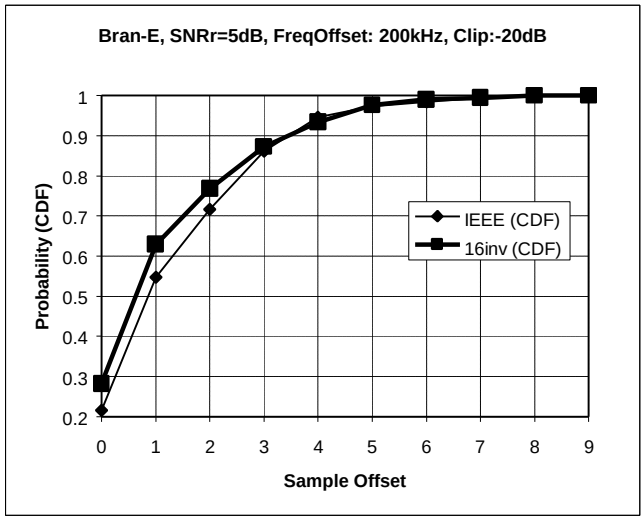

Figure 4-1 Timing acquisition accuracy measured in samples (Ch-E, 5dB, -20 dB clipping)

Conclusions and Recommendation

Using the structure given in Figure 2-2 gives the most accurate results in comparison to the currently proposed structure as shown in Figure 2-1. A reliable coarse timing in field A of the preamble can be achieved if the structure *A16inv* is used. Several drawbacks of the currently proposed A_field structure have been observed and it is shown that the false alarm and synchronisation failure rates are considerably higher as for *A16inv*. Furthermore a sequence is proposed for field *A16_inv* which achieves a low peak-to-mean-power-ratio, a small dynamic range and good performance.
Recommendation: Apply structure *A16_inv* to the A-field of the synchronisation preamble.

5 Abbreviations

CD____Correct Detection
DF____Detection failure
FA____False Alarm

6 References

[1] HL12ERI6A, BRAN12, 12.-15.01.99, Orlando
[2] 12PHY_MIN, BRAN12 PHY minutes
[3] "Criteria for Comparison" 30701F ETSI Project BRAN July 1998
[4] "High Performance Radio Access Local Area Networks – Type 2 (System Overview)", DTR/BRAN-00230002 v0.0.7, October 1998